

A DFT Study of CH_x Chemisorption and Transition States for C–H Activation on the Ru(1120) Surface

I. M. Ciobica* and R. A. van Santen

Schuit Institute of Catalysis, Eindhoven University of Technology, SKA, P.O. Box 513,
5600 MB Eindhoven, The Netherlands

Received: August 17, 2001; In Final Form: February 12, 2002

The thermodynamics of methane decomposition on the ruthenium (1120) surface has been investigated with *ab initio* periodic calculations. All surface intermediates are more stable than the gas-phase methane even if the last step of the decomposition path: $\text{CH} \rightarrow \text{C} + \text{H}$, is highly endothermic. Among all of the surface species, CH_2 appears to be the most stable. All of the surface species (CH_x , $x = 3-1$ and H) adsorb on bridge-up sites, while atomic C prefers top-down sites. The transition states of the elementary reactions for the dissociation of methane on the ruthenium (1120) surface have been investigated with nudged elastic band method (NEB). The calculated barriers are 56 kJ mol^{-1} for methane decomposition, 11 kJ mol^{-1} for methyl decomposition, and 52 kJ mol^{-1} for methylene decomposition, respectively. The decomposition of CH_{ads} requires the highest activation energy from the series with 95 kJ mol^{-1} .

1. Introduction

The reactivity of methane on metal surfaces is a catalytically important reaction. The sequential dehydrogenation of methane or the sequential hydrogenation of carbon are essential parts of the Fischer–Tropsch mechanism.

Several theoretical studies of methane activation and CH_x chemisorption on transition metal surfaces have been recently published based on results from *ab initio* calculations, none of those are on the (1120) or other open surfaces.

Yang and Whitten^{1,2} studied CH_x species on pure and substitutional Fe/Ni(111) using an embedded cluster technique. They found that CH_2 and CH species prefer hollow sites. A small barrier is present for the dissociation of $\text{CH}_2 \rightarrow \text{CH} + \text{H}$. The substitutional Fe/Ni(111) surface is more active for methane decomposition than for Ni(111); a barrier of only 24 kJ mol^{-1} is reported for the activation of CH_2 , compared to 70 kJ mol^{-1} for a clean Ni(111) surface.

Siegbahn and Panas studied CH_x chemisorption on the Ni(100) and Ni(111) surfaces using an *ab initio* cluster approach.³ They found that CH_x fragments have a similar stability on both Ni(100) and on Ni(111) surfaces. The vibrational C–H stretching frequencies computed for CH_x on Ni(100) are in good agreement with experimental results.

Burghgraef et al.^{4–7} studied methane activation on Co and Ni clusters using the density functional theory (DFT). Methane decomposition steps are found to be endothermic, except the transformation of $\text{CH}_2 \rightarrow \text{CH} + \text{H}$. A barrier of approximately 100 kJ mol^{-1} was reported for the CH_4 activation on these clusters.

Kratzer et al.⁸ studied methane dissociation on pure and on gold-alloyed Ni(111) surfaces using a periodic DFT approach. The rupture of the C–H bond occurs preferentially on a top Ni site, with a barrier of about 100 kJ mol^{-1} . The corresponding transition state have been taken from the cluster calculations of Burghgraef et al.⁴ with very similar energetic results.

Paul and Sauter^{9–11} studied the relative stability of CH_x species on Pd(111) with DFT slab calculations. The H, C, and CH species are found to prefer the hollow sites. CH_2 adsorbs on a bridge site while CH_3 is located on the atop site. The consecutive methane decomposition steps are endothermic except for the transformation of $(\text{CH}_2)_{\text{ad}}$ to CH_{ad} .

Au et al. and Liao et al.^{12,13} studied methane dissociation on Rh, Ni, Pd, Pt, and Cu (111) metal surfaces with and without preadsorbed atomic oxygen, using DFT with clusters as models for the transition metal surfaces. For the overall decomposition of methane to C_{ad} and H_{ad} , the energy is found to become less exothermic in the order $\text{Ni} < \text{Pd} \approx \text{Pt}$, while for Cu the overall dissociation reaction is endothermic. Chemisorbed atomic O on the unstable atop sites promotes methane dissociation on Ni, Pd, Pt, and Cu, while atomic O on a hollow site promotes methane dissociation only on Cu.

Newer results from the same group¹⁴ show the adsorption energies and the transition states for methane dissociation and syngas formation on Ru, Os, Rh, Ir, Pd, Pt, Cu, Ag, and Au clusters with DFT. Methane is very weakly adsorbed on all metal surfaces and the CH_x species are more strongly adsorbed as the number of H atoms bound to C is decreasing. The barriers for $\text{CH}_x \rightarrow \text{CH}_{x-1} + \text{H}$ are between 60 and 200 kJ mol^{-1} .

Using TPD, H/TPD, AES, and HREELS Wu et al.^{15,16} have observed CH, CCH_2 , and CCH_3 , as well as graphitic carbon on Ru(0001) and Ru(1120) with methane at 5 Torr for 120 s. The apparent activation energy for methane dissociation is found to be around 36 kJ mol^{-1} on the Ru(0001) surface. In the same group, methane coupling at low temperature on Ru(0001) and Ru(1120) catalysts was investigated.¹⁷ For the Ru(0001) surface a maximum yields of ethane and propane is observed at $T_{\text{H}_2} = 400 \text{ K}$, whereas for Ru(1120) no maximum was found. The same three species were observed on both surfaces with HREELS, as was done in previous experiments. Only on the Ru(1120) surface ethylidyne was detected below $T_{\text{CH}_4} = 400 \text{ K}$.

Guczi et al.¹⁸ present a low-temperature methane activation under nonoxidative conditions over supported Ru–Co bimetallic system. A method of deuterium uptake by the surface CH_x

* To whom correspondence should be addressed. E-mail: I. M.Ciobica@TUE.nl.

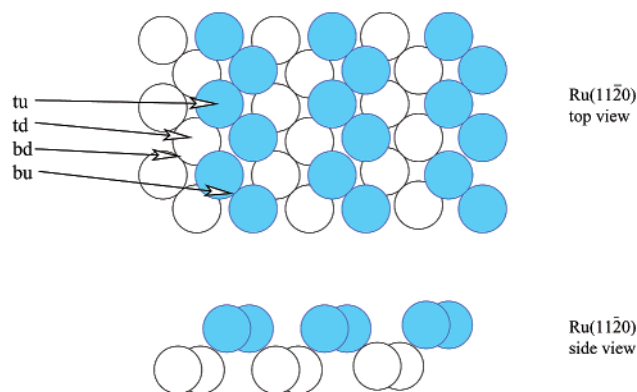


Figure 1. Top and side view of the ruthenium (11 $\bar{2}$ 0) surface.

species formed after CH₄ dissociation is used to determine the H content in adsorbed CH_x species. On Ru–Co/SiO₂ and Ru–Co/NaY[II], the ratio CHD₃/CD₄ is larger than 1 and decreases with the increase of the temperature. On Ru–Co/Al₂O₃ and Ru–Co/NaY[I] (O₂ treated), the same ratio is smaller than 1 and increases with the increase of the temperature. The amount of CH₃D is very small for all supports, and CH₂D₂ is present in quantities usually smaller than CHD₃ and CD₄ quantities.

This paper presents the thermodynamics of adsorbed CH_x species ($x = 0-4$) on the ruthenium (11 $\bar{2}$ 0) surface as well as the transition states for each elementary reaction for CH_x ($x = 1-4$) decomposition to CH_{x-1} ($x = 1-4$) and H atom in a similar way to that we used for the ruthenium (0001) surface.^{19,20}

2. Method and Surface Model

This quantum chemical study was performed using the VASP^{21,22} code, which performs periodic ab initio DFT calculations using pseudopotentials and a plane wave basis set. The approach implemented in the program is based on a finite-temperature-generalized gradient approximation with the Perdew Wang 91 functional.²³ The interaction between ions and electrons is described using the ultrasoft pseudopotentials (US-PP) introduced by Vanderbilt²⁴ and provided by Kresse and Hafner.²⁵

The surface model consists of a super cell with a slab of eight metal layers and 10 layers of vacuum between the surfaces. This may seem a lot, but it is just the same amount we used for the Ru(0001) surface before.^{19,20} This surface is more open (see Figure 1), first two layers are both exposed to the vacuum. The atoms on the first layer have seven neighbors and the atoms from the second layer have 11 neighbors. (For the (0001) surface, each atom from the first layer has nine neighbors.)

Adsorption on both sides with an inversion center avoids the generation of dipole–dipole interactions between the cells. Cells with 1×1 structures are considered (corresponding to 50% coverage) (see Figure 1).

The geometries of the surface and of the adsorbates are fully optimized. Intermediates have been studied on the four different sites for H atom and CH_x ($x = 1-3$) species: atop up (tu), atop down (td), bridge up (bu), and bridge down (bd). The atop-up and bridge-up adsorption modes involve only atoms from the first metal row, which are the ones more unsaturated. Atop-down and bridge-down adsorption modes involve not only atoms from the second row, but also from the first row. The atop-down adsorption mode is in fact a fifth-fold adsorption mode (one atom from the second row and four atoms from the first row), the adatom being at more or less the same height as the metal atoms from the first layer. The bridge-down adsorption

mode is 4-fold adsorption mode (two atoms from the second layer (short bridge) and two atoms from the first row (long bridge)), the adatom being also more or less at the same height as the metal atoms from the first layer. In Figure 1 the adsorption sites are shown. Since hollow sites are not present on this particular surface, the adsorption energies of CH_x are expected to be lower, even if the surface is more reactive!

The k-points sampling was chosen with respect to the symmetries of the system following the Monkhorst–Pack procedure.²⁶

The NEB Method²⁷ developed by Jónsson et al. is implemented in vasp.4.4 code. The main difference between NEB and elastic band (EB) method²⁸ is that on NEB the perpendicular component of the spring force and the parallel component of the true force are projected out. Both methods are chain-of-states methods: two points in the hyperspace containing all the degrees of freedom are needed and a linear interpolation can be made to produce the images along the elastic band. The program will run simultaneously each image and will communicate at the end of each ionic cycle in order to compute the force strings.

Also in NEB, a smooth switching function is introduced that gradually turns on the perpendicular component of the spring force where the path becomes kinky at large differences in the energies between images.

Practically, this method requires large parallel computer resources and its success depends on input strategies (starting images) and careful monitoring of the process.

The quasi-Newton algorithm,²⁹ used to refine the obtained result with NEB, implies that the atoms are moved according to the minimization of the forces, no criteria for minimizing the total energies is added. In this way the program is searching a stationary point. Only in the very few cases when the given initial geometry is close to the geometry of the transition state we can reach it with the quasi-Newton technique, so the NEB is still required to search the transition states.

3. Results

We will discuss first the relative stability of each CH_x species on all adsorption sites, then we will discuss the coadsorption with H atom, and finally the transition states for elementary reactions of CH_x decomposition will be analyzed.

3.1. Adsorbed CH_x ($x = 4-0$). *Adsorbed CH₄.* Methane is weakly adsorbed. Our experience with Ru(0001) shows that methane is physisorbed with -1 kJ mol^{-1} for 25.0% coverage and -3 kJ mol^{-1} for 11.1% coverage. On the (11 $\bar{2}$ 0) surface the picture is similar, all adsorption modes have a negligible adsorption energy. The metal–H distance is 2.5 \AA for the case of adsorbed methane with one H atom pointing down to the surface. All C–H bond length are about 1.1 \AA : the methane molecule is not distorted.

Adsorbed CH₃. Methyl molecules prefer to adsorb on the bridge-up position. The adsorption energy with respect to gas-phase methyl and bare metal surface is -221 kJ mol^{-1} . The atop-up adsorption mode is less stable with 21 kJ mol^{-1} . This can give us some information about the mobility of methyl species on this particular surface.

All C–H bonds are 1.1 \AA , and HCH angles are 111° and two times 104° for the stable adsorption mode and three times 109° for the metastable adsorption mode. C–Ru distances are 2.1 \AA and 2.3 \AA for bridge-up adsorption and 2.1 \AA for atop-up adsorption. Ru–C–Ru angle is 74° , and one H atom is at a distance of 2.0 \AA from a metal atom in the case of the bridge-up adsorption mode. The atop-up geometry is slightly tilted.

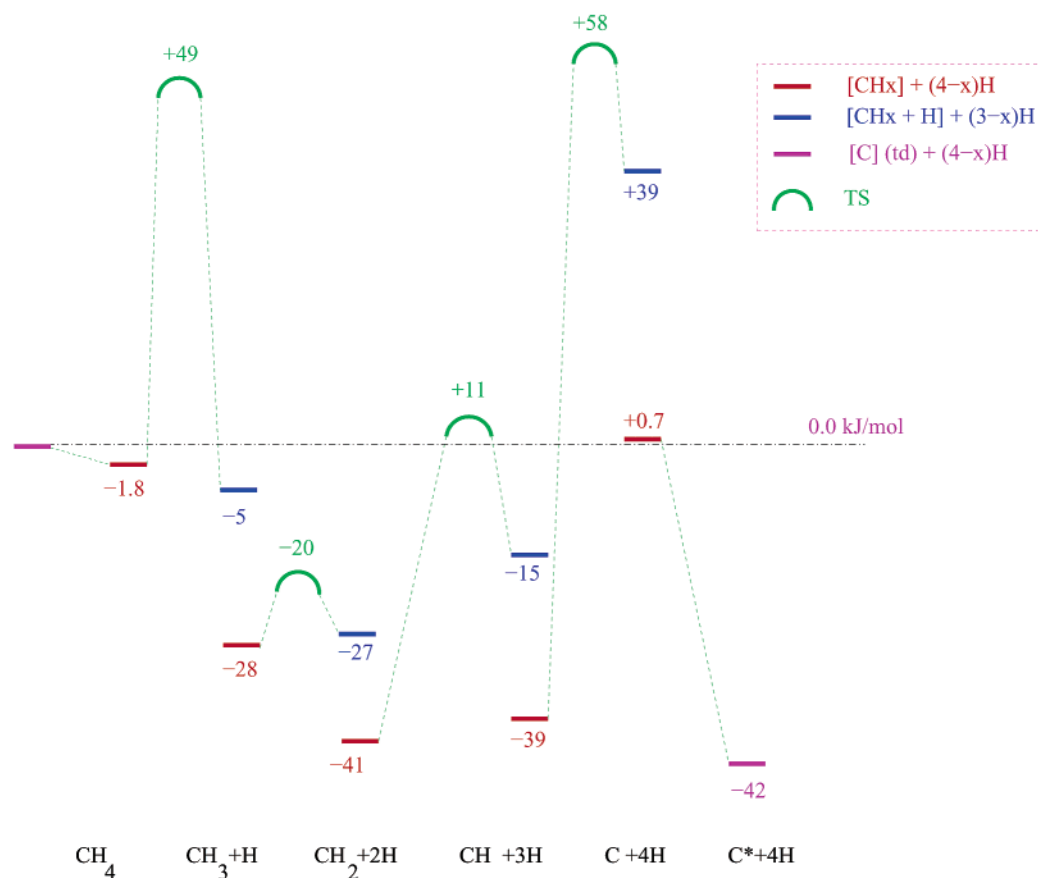


Figure 2. Full path for methane activation on the Ru(11 $\bar{2}$ 0) surface.

Top-down and bridge-down adsorption modes are not stable: during the optimization the atoms move toward the most stable bridge-up configuration.

Adsorbed CH₂. Methylene molecules also prefer to adsorb on the bridge-up position. The adsorption energy with respect to gas-phase methylene and bare ruthenium surface is -439 kJ mol^{-1} . We were not able to identify a stable atop up adsorption mode, since methylene got dissociated to adsorbed CH and adsorbed H. However, we managed to compute a metastable top-down adsorption mode as being 19 kJ mol^{-1} less stable. Also, methylene seems mobile on this surface.

Among all other species, methylene is the most stable from the CH_x series. This result is different compared with the (0001) surface.

The C–H bonds are 1.1 \AA , and H–C–H are 113° for bridge-up and 101° for top-down adsorption modes. The C–Ru bond lengths are both 2.1 \AA in the case of the bridge-up configuration, and for top down we have 2.1 \AA for the Ru atom on the second layer, $2.1, 2.3,$ and 2.9 \AA for three Ru atoms from the first layer from one row and 2.6 \AA for the fourth metal atom from the first layer from an other row. This bridge-down configuration has the H atoms from adsorbed CH₂ close to metal atoms from the first row. The distances are 2.3 \AA for one H atom and 2.5 and 2.0 \AA , respectively, for the other H atom.

Adsorbed CH. Methyn molecules also prefer the bridge-up configuration for adsorption. With respect to bare ruthenium surface and gas-phase CH, the adsorption energy is -624 kJ mol^{-1} . The top-down, slightly distorted configuration is less stable with 45 kJ mol^{-1} , and next is the tilted atop-up adsorption mode with 96 kJ mol^{-1} . This species has a limited mobility compared with methyl and methylene.

The relative stability of CH is close to that for CH₂.

The C–H bond length is 1.1 \AA , the C–Ru bond lengths are twice 1.9 \AA for bridge up, 2.1 \AA ; for Ru_{down}–C in top-down adsorption mode, $2.1, 2.0,$ and 2.6 \AA for Ru_{up}–C; and 2.9 \AA for Ru_{up}–C from the other row, respectively. The C–Ru distance for atop-up adsorption mode is 1.7 \AA . The Ru–C–Ru for bridge-up adsorption is 91° . H–C–Ru angle for top down is 139° , and for atop up is 178° .

The bridge-down adsorption mode leads to a distortion of the metal layers.

Adsorbed C. Atomic C behaves a bit different like all CH_x. It prefers to adsorb in the tilted top-down configuration. With respect to bare metal surface and gas-phase atomic carbon, the adsorption energy is -709 kJ mol^{-1} . The next local minima is for bridge-up adsorption mode, less stable with 43 kJ mol^{-1} ! It is followed by bridge down with 127 kJ mol^{-1} less stable, and by top up with 160 kJ mol^{-1} .

The Ru_{down}–C distance is 2.0 \AA ; the Ru_{up}–C distances are $2.0, 1.9,$ and 2.5 \AA , respectively, for one row; and 2.9 \AA for the other row in the case of top-down adsorption mode. The bridge-up configuration has two distances of 1.9 \AA , bridge-down has Ru_{down}–C bond lengths of 2.1 \AA , while Ru_{up}–C bond lengths are 1.9 \AA . The top-up adsorption mode has a C–Ru bond length of 1.7 \AA . Ru–C–Ru angles are 97° for bridge up, and for bridge down we have a Ru_{down}–C–Ru_{down} angle of 79° and a Ru_{up}–C–Ru_{up} angle of 160° .

Adsorbed H. The H atom adsorbs on the bridge-up configuration. With respect to H₂ molecule in gas phase and bare Ru surface, the adsorption energy is -54 kJ mol^{-1} . Top-up and top-down are not stable adsorption modes: during the optimization H atom is moving toward the more stable bridge-up geometry. Bridge-down is metastable, less stable with 172 kJ mol^{-1} .

TABLE 1: Absolute Values Relative to the CH_x in Gas Phase and the Bare Metal Surface for the Most Stable Adsorption Modes^a

	species				
	CH ₃	CH ₂	CH	C	H
adsorption site	bu	bu	bu	td	bu
energy (kJ mol ⁻¹)	-221.3	-439.2	-624.2	-675.4	-53.9

^a “bu” is bridge-up, and “td” is atop-down.

The H–Ru bond lengths are twice 1.8 Å for bridge up and four times 2.0 Å for bridge down. The Ru–H–Ru angles are 99° for bridge up and 83° for Ru atoms in the second layer, and 163° for Ru atoms in first layer, respectively.

3.2. Coadsorption of CH_x ($x = 0-3$) with Atomic H. In all those calculations we considered that H and CH_x ($x = 0-3$) are adsorbed in bridge-up configurations. Other combinations were not tested since we believe that at this coverage it is not possible.

CH₃ and H. To coadsorb an H atom close to a adsorbed methyl on the Ru(11 $\bar{2}$ 0), surface costs about 23 kJ mol⁻¹. This is more than that in the case of the coadsorption on the Ru(0001) surface. We can explain this by a higher coverage on the Ru(11 $\bar{2}$ 0) surface and the large volume of the methyl group. The geometry of adsorbed methyl is not changed, the most affected is the H atom, which now has two asymmetric Ru–H bonds of 1.8 and 2.0 Å with the two Ru atoms from the first layer, and also it approaches one atom from the second layer at the distance of 2.0 Å. The distance H–CH₃ is 2.8 Å.

CH₂ and H. The coadsorption of a H atom with a methylene reduces the adsorption energy with 14 kJ mol⁻¹. This is similar to the repulsion in the case of coadsorption on the (0001) surface. Also, the neither geometry of methylene nor of H is affected by the coadsorption. The distance H–CH₂ is 2.3 Å.

CH and H. The lateral interaction between adsorbed CH and adsorbed H is repulsive and about 24 kJ mol⁻¹. This is more than that for CH₂ since CH adsorbs more strongly. Because of the symmetry constraints, the structures of adsorbed CH and adsorbed H do not differ from those adsorbed separately. The distance H–CH is 2.2 Å.

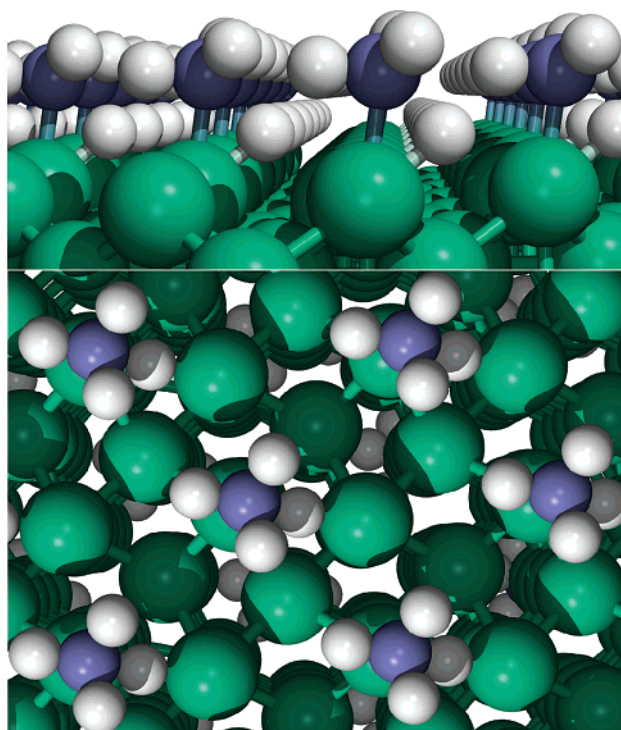
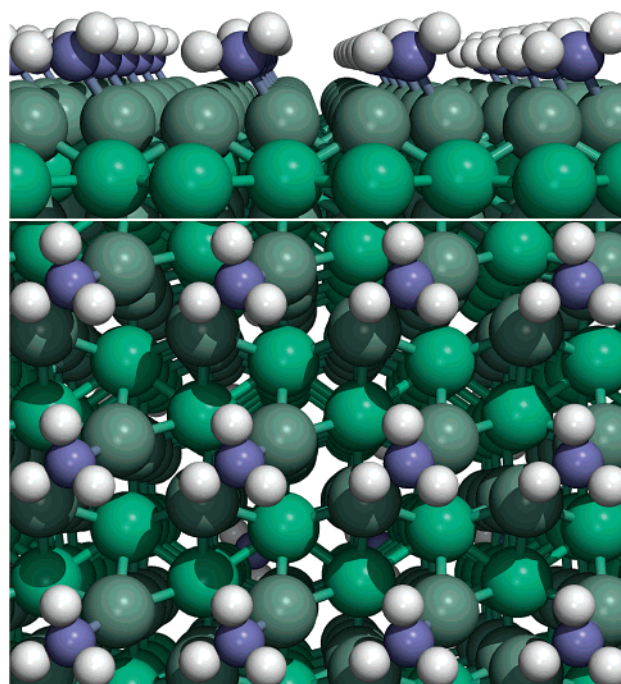
C and H. The lateral interaction between adsorbed C and H is larger than the one for CH: it is 39 kJ mol⁻¹. Similar to CH and H coadsorptions, C and H have a geometry like the separate adsorptions. The distance H–C is also 2.2 Å.

3.3. Transition States for Elementary Reactions. The energies of the CH_x ($x = 3-1$) species adsorbed in the most stable site, as well as the transition states are presented in Figure 2. Absolute values relative to the CH_x in gas phase and the bare metal surface (also optimized) for the most stable adsorption modes are given in Table 1.

CH₄ → CH₃ + H. The barrier for methane activation on Ru(11 $\bar{2}$ 0) we report here is 56 kJ mol⁻¹. This is smaller than that for the Ru(0001) surface. This can be explain by the higher coverage and by the lesser neighbors for the Ru atoms involved in the reaction. The transition state is a very early one, the same as that for Ru(0001).

The activated H atom is at 1.5 Å from the C atom. The other H atoms have H–C bond lengths of 1.1 Å. The angles H–C–H are 110° for the normal H atoms, and between 83° and 96° for one H atom activated. The C–Ru distance is 2.2 Å. The Ru–H bond lengths for the activated H atom are 1.9 and 1.8 Å. The Ru–H–Ru is 99°. See Figure 3.

There are some similarities between this TS and the same for the close packed surface of ruthenium. Both are with the C atom atop site and with the activated H atom in a nonsymmetric bridge site.

**Figure 3.** The early TS structure for methane decomposition on the Ru(11 $\bar{2}$ 0) surface.**Figure 4.** The early TS structure for methyl decomposition on the Ru(11 $\bar{2}$ 0) surface.

CH₃ → CH₂ + H. The activation of methyl is a easy process, similar to the activation of methylene on the Ru(0001) surface. The barrier is just 11 kJ mol⁻¹. The activated H atom is at 1.2 Å from the C atom, while the other C–H bond lengths are still 1.1 Å. The angle H–C–H between the nonactivated H atoms is 111°, while between the activated H atoms they are 101° and 106°. The CH₃ group is still in the bridge site with C–Ru bonds of 2.2 Å and 2.3 Å, the Ru–C–Ru angle being 74°. The activated H atom is on-top a metal atom at a distance of 2.0 Å. See Figure 4.

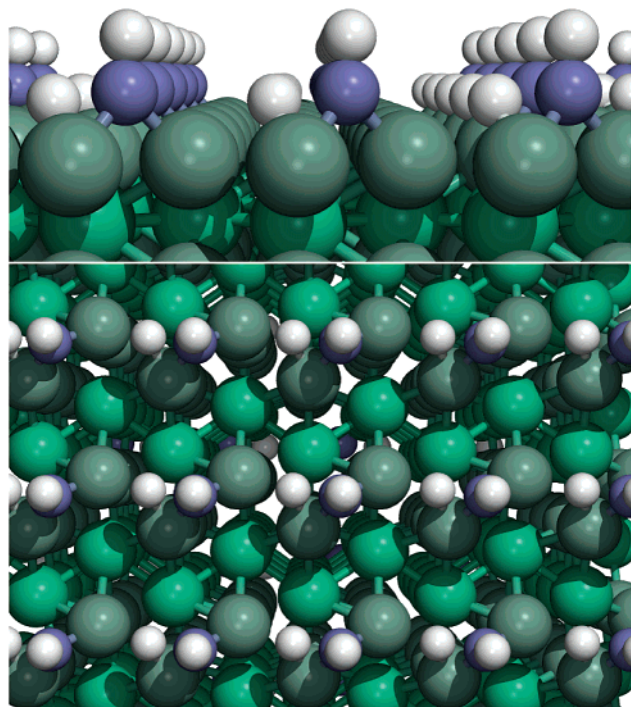


Figure 5. The TS structure for methylene decomposition on the Ru(1120) surface.

There are certain similarities between this transition state and the transition state for methylene decomposition on the (0001) surface. Here, because of the decomposition of CH_3 , it results in the most stable species. One H is already activated due to the geometric constraints (one H is on-top a metal atom). CH_2 on the (0001) surface will also give by decomposition the most stable species from that series: one H is also activated due to geometric constraints (one H is on-top a metal atom).

$\text{CH}_2 \rightarrow \text{CH} + \text{H}$. The activation of the most stable intermediates requires 52 kJ mol^{-1} . The activated H atom is at 1.5 \AA from the C atom, and it is in a tilted bridge-up position at 1.8 and 2.1 \AA , respectively. The remaining CH group is in the initial bridge up configuration, with 2.0 and 1.9 \AA C–Ru bond lengths (in between Ru– C_{CH} and Ru– C_{CH_2}). The angle Ru–C–Ru is 62° , the angle H–C–H is 99° , and the angle Ru–H–Ru for the activated H atom is 87° . See Figure 5.

$\text{CH} \rightarrow \text{C} + \text{H}$. The activation of CH require the largest amount of energy from the CH_x series on the Ru(1120) surface, 95 kJ mol^{-1} . The activated H atom is also at 1.5 \AA from the C atom: the CH is parallel with the surface in this late transition state. The Ru–H bond lengths are 1.8 and 2.0 \AA . The Ru–C bond lengths are 1.8 \AA and 1.9 \AA . The Ru–C–Ru angle is 95° , and the Ru–H–Ru angle is 89° . See Figure 6.

Conclusions

Adsorbed methyl and adsorbed methylene are mobile on the Ru(1120) surface, while CH and C present a limited mobility. All species are more stable on the bridge up adsorption mode, except for adsorbed C, where the tilted top-down adsorption mode is, with 9 kJ mol^{-1} , more stable. Since those calculations are for 50% coverage, we expect some important lateral interactions especially for C and CH. Compared to the close packed surface, all species have smaller adsorption energies, and we assume that this is due to the particularity of the surface which has no 3-fold sites for adsorption.

Methylene is the most stable species from the adsorbed CH_x series ($x = 0$ –3) on the (1120) surface, while on the (0001) surface adsorbed CH was by far the most stable species.

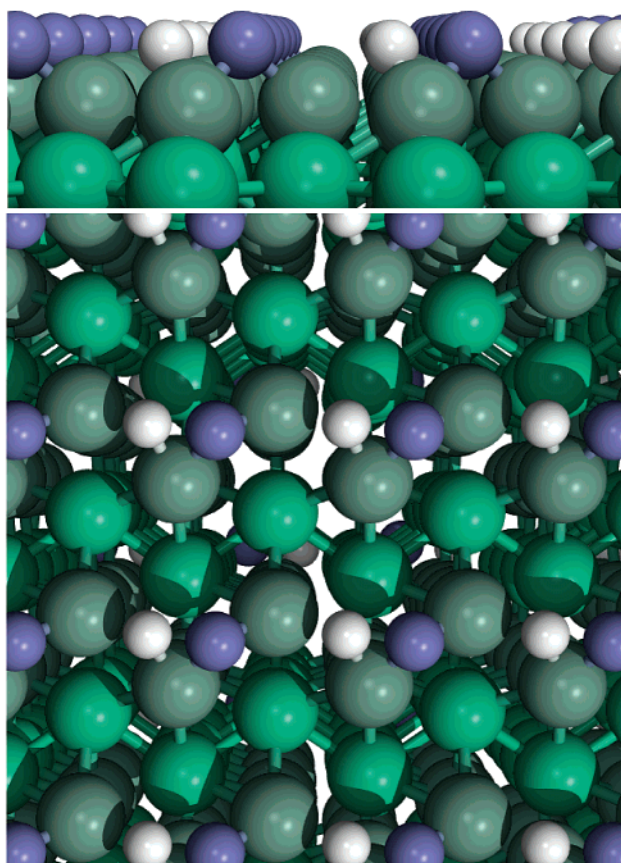


Figure 6. The late TS structure for methyne decomposition on the Ru(1120) surface.

H coadsorption with CH_x ($x = 0$ and 3) is repulsive. The smallest one is in the case of methylene, which do not have a large volume as methyl and also not a strong adsorption as CH or C.

Transition states for C–H activation on Ru(1120) are different from the ones on Ru(0001). Similarities are in the cases $\text{CH}_4/(1120)$, $\text{CH}_2/(0001)$ with $\text{CH}_3/(1120)$, and $\text{CH}/(0001)$ with $\text{CH}/(1120)$. The activation of methane and methyl are early transition states, while the activation of CH is a late transition state.

The decomposition of methane, methylene, and methyn have the activated H atom in a bridge site and a C–H distance of 1.5 \AA . On the (0001) surface, the decomposition of methyl and methyn have the activated H ontop a metal atom at the distance of 1.6 \AA from the C atom. The decomposition of methyl is different. A shorter C–H distance of 1.2 \AA for the activated H atom indicates an early transition state.

The Ru(1120) surface is a more open surface compared with the Ru(0001), and more reactive. The CH_x species are strongly bonded to the surface, but less than in the case of the Ru(0001) surface. This can be interpreted as inconsistent, but the explanation is that the CH_x species prefer to adsorb on 3-fold hollow sites, which are absent on the Ru(1120) surface. The CH_x species are more reactive on the Ru(1120) surface compared with the CH_x species adsorbed on bridge sites on the Ru(0001) surface. This make the CH_x species even more reactive than the CH_x species on hollow sites from the Ru(0001) surface.

Acknowledgment. This work is part of the research program of the “Stichting voor Fundamenteel Onderzoek der Materie (FOM)”, which is financially supported by the “Nederlandse organisatie voor Wetenschappelijke Onderzoek (NWO)”. This

work has been accomplished under the auspices of NIOK, the Netherlands Institute for Catalysis Research, Lab Report No. TUE-2001-5-3. The calculations have been partially performed with NCF support (SC183 and MP43b).

References and Notes

- (1) Yang, H.; Whitten, J. L. *Surf. Sci.* **1993**, 289, 30.
- (2) Yang, H.; Whitten, J. L. *J. Chem. Phys.* **1989**, 91, 1, 126.
- (3) Siegbahn, P. E. M.; Panas, I. *Surf. Sci.* **1990**, 240, 37.
- (4) Burghgraef, H.; Jansen, A. P. J.; van Santen, R. A. *Surf. Sci.* **1995**, 324, 345.
- (5) Burghgraef, H.; Jansen, A. P. J.; van Santen, R. A. *Faraday Discuss.* **1993**, 96, 337.
- (6) Burghgraef, H.; Jansen, A. P. J.; van Santen, R. A. *Surf. Sci.* **1995**, 344, 149.
- (7) Burghgraef, H.; Jansen, A. P. J.; van Santen, R. A. *J. Chem. Phys.* **1994**, 101, 12, 11012.
- (8) Kratzer, P.; Hammer, B.; Nørskov, J. K. *J. Chem. Phys.* **1996**, 105, 13, 5595.
- (9) Paul, J.-F.; Sautet, P. *J. Phys. Chem. B* **1998**, 102, 1578.
- (10) Paul, J.-F.; Sautet, P. In *Proceedings of the 11th International Congress on Catalysis—40th Anniversary Studies in Surface Science and Catalysis*; Hightower, J. W., Delgass, W. N., Iglesia, E., Bell, A. T., Eds.; Elsevier Science B.V.: Amsterdam, 1996; Vol. 101, p 1253.
- (11) Paul, J.-F.; Sautet, P. Symposium Advances and Applications of Computational Chemical Modeling to Heterogeneous Catalysis. Presented Before the Division of Petroleum Chemistry, Inc. 213th National Meeting, American Chemical Society, San Francisco, CA, April 13–17, 1997.
- (12) Au, C.-T.; Liao, M. S.; Ng, C. F. *Chem. Phys. Lett.* **1997**, 267, 44.
- (13) Liao, M. S.; Au, C.-T.; Ng, C. F. *Chem. Phys. Lett.* **1997**, 272, 445.
- (14) Au, C.-T.; Ng, C. F.; Liao, M. S. *J. Catal.* **1999**, 185, 12.
- (15) Wu, M.-C.; Goodman, D. W. *J. Am. Chem. Soc.* **1994**, 116, 1364.
- (16) Wu, M.-C.; Goodman, D. W. *Surf. Sci. Lett.* **1994**, 306, L529.
- (17) Lenz-Solomun, P.; Wu, M.-C.; Goodman, D. W. *Catal. Lett.* **1994**, 25, 75.
- (18) Gucci, L.; Sarma, M. V.; Borkó, L. *J. Catal.* **1997**, 167, 495.
- (19) Ciobica, I. M.; Frechard, F.; van Santen, R. A.; Kleyn, A. W.; Hafner, J. *Chem. Phys. Lett.* **1999**, 311, 185.
- (20) Ciobica, I. M.; Frechard, F.; van Santen, R. A.; Kleyn, A. W.; Hafner, J. *J. Phys. Chem. B* **2000**, 104, 3364.
- (21) Kresse, G.; Furthmüller, J. *Comput. Mater. Sci.* **1996**, 6, 15.
- (22) Kresse, G.; Furthmüller, J. *Phys. Rev. B* **1996**, 54, 16, 169.
- (23) Perdew, J. P. *Electronic Structure of Solids, 1991*; Akademie Verlag: Berlin, 1991.
- (24) Vanderbilt, D. *Phys. Rev. B* **1990**, 41, 7892.
- (25) Kresse, G.; Hafner, J. *J. Phys.: Condens. Matter* **1994**, 6, 8245.
- (26) Monkhorst, H. J.; Pack, J. D. *Phys. Rev. B* **1976**, 13, 5188.
- (27) Jónsson, H.; Mills, G.; Jacobsen, K. W. In *Classical and Quantum Dynamics in Condensed Phase Simulations*; Berne, B. J., Ciccotti, G., Coker, D. F., Eds.; World Scientific: River Edge, NJ, 1998.
- (28) Pratt, L. R. *J. Chem. Phys.* **1986**, 85, 5045.
- (29) Pulay, P. *Chem. Phys. Lett.* **1980**, 73, 393.